Multi-Band Transparent Optical Network Planning Strategies for 6G-Ready European Networks

Sai Kireet Patri[a,b,*], Achim Autenrieth[a], Jörg-Peter Elbers[a], Carmen Mas-Machuca[b]

[a] *ADVA, Fraunhoferstr. 9a, Martinsried/Munich, Germany*
[b] *Chair of Communication Networks, TU Munich, Arcisstr. 21, Munich, Germany*

Abstract

As long-haul network operators upgrade core optical networks to support 5G services, research and standardization efforts for 6G have begun. Keeping in mind the ever-growing demand for high-bandwidth services, our work proposes a novel core-network traffic model which exploits the network's graph and population metric to estimate demands. We further develop a multi-period Routing, Configuration, and Spectrum Assignment (RCSA) algorithm which takes as input the traffic model demands, and provides network metrics spread across all planning periods.

A multi-period multi-band transparent optical network planning study on three European networks is undertaken, using two deployment approaches; namely, flexible bandwidth variable transceivers (Flex-BVTs) and transparent IP over wavelength division multiplexing (IPoWDM). We show that Flex-BVT places up to 15% lesser equipment into the network while carrying up to 20% higher traffic. Using a simple Capital Expenditure (CAPEX) calculation, we also show that the CAPEX-per-bit of deploying Flex-BVTs is up to 12% lower, as compared to transparent IPoWDM solutions.

Keywords: Optical Networks, Traffic Model, Network Planning, BVT, Transparent IPoWDM, CFP2DCO

2020 MSC: 90C27, 90C35, 05C85

*Corresponding author
Email address: SPatri@adva.com (Sai Kireet Patri)

1. Introduction

Under European Commission's guidelines, national and continental network operators in Europe have already begun 5G deployment, with a vision to provide high bandwidth mobile services to all urban and transportation users by 2025 [1]. Meanwhile, bandwidth-hungry services being offered to both residential and business users are placing network operators in an 'upgrade or perish' situation [2]. Recent trends in communication networks research getting fiber as close to the Customer Premise Equipment (CPE) as possible, as shown in Fig. 1. Due to the ability of access networks to support client rates of up to 40 Gbps, core networks connecting different regions of a country, need to be sufficiently upgraded too. Adding to this, the global chip shortage and inflation have increased the relevance to reduce the overall cost per bit for core network operators [3].

In the coming years, it is forecasted that core network traffic will keep increasing, and previous methods of over-provisioning by leasing additional dark fibers may become expensive [4]. Network operators, therefore, need to exploit the availability of software tunable Flex-BVTs, along with the possibility to use the low attenuation regimes of the C-, L-, and S-Bands to extract the maximum possible capacity from each fiber in their network. Such an approach is necessary to ensure that networks across Europe are ready not only to meet requirements set by the European Commission but also to be ready for 6G services rollout in the future.

1.1. Capacity Upgrade Solutions

As standardization bodies and researchers have already begun efforts to define latency and bandwidth requirements for services in the 6G ecosystem, core network operators need to plan a budget for network investments to have sufficient capacity provisioned when the need arises. There are several commercial

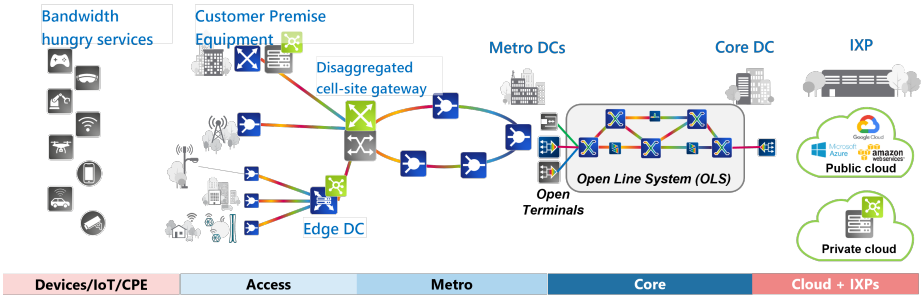

Figure 1: Optical Networks in the current network ecosystem. Our work focuses on core networks providing connectivity to DCs and IXPs.

offerings available from optical transport network vendors, which can be utilized by network operators to scale their capacities, including optical terminal equipment upgrade [5].

Another way of increasing capacity is to use IP over Wavelength Division Multiplexing (IPoWDM) pluggables which can convert 100, 200, and 400 GbE client rates directly to 100, 200, or 400 Gbps optical signals. Specifically, for transparent long-haul applications, the OpenROADM-based 100G Form Factor Pluggable 2- Digital Coherent Optics (CFP2-DCO) modules provide an alternative to Flex-BVT-based deployment [6]. These modules can connect directly to a high-speed switching router which can further be connected to the Open Line System (OLS).

At the OLS layer, transparent IPoWDM has emerged as a cost-effective competitor to the Flex-BVT-based deployments; however, higher costs related to coherent optics-enabled routers, and the versatility of Flex-BVTs must also be considered in an upgrade decision. Moreover, as shown in Table 1, multi-haul CFP2-DCO modules can achieve a maximum of 16 QAM and 64 GBaud configurations. An 'a-la carté' deployment of IPoWDM and Flex-BVTs might result in the best of both worlds and eventually lower capital expenditure than pure deployments; although network operations, maintenance, and logistical cost of such an approach still need to be adequately studied.

Network operators need to evaluate these terminal upgrade solutions to make

Sl. No.	Technology	Datarate (Gbps)	Modulation Formats	Baud Rate (GBaud)
1	Flex-BVT	100-600	QPSK-64QAM	28-72
2	CFP2-DCO	100-400	QPSK-16QAM	28-64

Table 1: Comparison of differences between Flex-BVTs and CFP2-DCO in terms of optical performance

strategic investment decisions for a future-proof provisioned network capacity. Moreover, as wide-band low noise figure Erbium Doped Fiber Amplifier (EDFA) and Thulium Doped Fiber Amplifier (TDFA) technologies mature, these may soon be included in commercial network deployment. The question therefore arises, as to how soon must a network operator deploy a multi-band solution. Adding additional bands is a cost-intensive exercise, due to the addition of band splitters and combiners at each amplification point in the network. However, several studies have shown that such an investment is bound to be cheaper than lighting additional dark fibers while offering similar growth in carried traffic [7, 8].

1.2. Contributions

In our work, we first propose a traffic model relevant to transparent optical core networks of the future. Then, using this traffic model, we conduct a multi-period network planning study by enabling C, L, and S bands and comparing two distinct deployment solutions (Flex-BVT and CFP2-DCO) on three long-haul networks. Finally, we envision a simple cost model and compare the overall CAPEX of the two solutions spread across the planning periods.

The rest of the paper is organized as follows: In Section 2 we look at the state-of-the-art approaches to increase optical network capacity. Subsequently, in Section 3 we define how future multi-band optical networks could be deployed in long-haul transparent networks. Then, in Sections 4 and 5 we discuss in detail our contributions to the traffic generator and the network planning algorithms respectively. These algorithms are further used for network studies and techno-economic analysis in Section 6. Finally, we summarize our work with Section 7

and provide an outlook for the future direction of our work.

2. State of the Art

Over the past decade, several transmission experiments have been undertaken to increase the traffic carried by a single fiber. Of these, two broad methods were, *i)* increasing the total number of frequency slots by exploring the S- and L-Bands, or *ii)* increasing the modulation rate of a transceiver, to achieve higher data rates per frequency slot.

Early works of exploring L- and S-Bands were able to transmit 32 10 Gbps non-return to zero Amplitude Key Shifted (NRZ-ASK) signals over 160 km of Non-Zero Dispersion Shifted Fiber (NZDSF) across the S-, C-, and L-Bands [9]. With the introduction of Dual Polarized Quarternary Phase Shift Keying (DP-QPSK) signals, a record transmission of 160 Wavelength Division Multiplexing (WDM) channels, spread across the C- and L-Bands over 240 km was shown [10]. Despite these seminal works, communication equipment manufacturers failed to add such capabilities to their product inventories, as the overall demand for such a solution was assumed to be low. A few years later, early works exploited advances in coherent detection using digital signal processing (DSP) to achieve record transmission of 200G Dual Polarized 16 Quadrature Amplitude Modulation (DP 16-QAM) signals, achieving 69.1 Tbps C+L-Band transmission over low-loss pure silica core fibers [11].

Given the pre-deployed C-Band Erbium Doped Fiber Amplifiers (EDFAs), the research on increasing transceiver capacity led to the development of Flex-BVTs. An architecture of a sliceable Flex-BVT that could achieve up to 400 Gbps 16-QAM signals was proposed [12]. With further advances in DSP, and the standardization of ITU-T flex-grid frequency slots, the interest in conducting network studies that exploited these characteristics also increased. Multi-layer network planning studies with a flex-grid deployment proved to hold several advantages over fixed-grid deployments [13, 14]. A techno-economic planning study with Flex-BVTs up to 400 Gbps 16-QAM was also undertaken, which

showed more than 50% savings on equipment cost as compared to fixed-grid deployments [15]. However, most of these studies were aimed at maximizing the C-Band capacity, with minimal focus on realistic network traffic increase, and the option of using frequency slots outside of the C-Band.

In recent years, IPoWDM-based solutions, namely QSFP-DD and multi-haul CFP2-DCO have emerged as a competitor to Flex-BVT-based solutions [16]. Within IPoWDM, there exist two methods of network design, namely, an opaque network design (using QSFP-DD-based pluggables) and a transparent network design (using multi-haul CFP2-DCO). For long-haul core networks, network studies were conducted based on the number of transceivers, and multi-haul CFP2-DCO emerged to provide a better cost per throughput in such networks [17, 18]. However, these studies ignore the fact that most IP routers do not have CFP2-DCO cages, which would force network operators to invest in routers which support multi-haul CFP2-DCO-based coherent routing [19].

Since operators are facing an exponential increase in traffic, network deployment studies focus on expanding to multiple bands instead of lighting additional dark fibers [20, 21]. With similar methodologies and tools, these studies look at maximizing the amount of traffic carried in each band, while focusing on power control and network upgrade strategies. Although network studies are indeed carried out with due diligence, particularly modelling the physical layer impairments accurately, the Flex-BVTs are mostly limited to 400 Gbps and the traffic model is either randomized or assumes a uniform joint probability distribution function.

Although network capacity studies have traditionally assumed Poisson arrival of lightpath requests to achieve progressive loading, these scenarios rarely give actionable inputs to network operators, since realistically, network traffic exchanged is skewed in favour of well-connected nodes with higher population [22, 23]. Due to the lack of open-source network data, it is difficult to make assumptions about the required traffic in each network. Machine learning has also been shown to be used for traffic prediction in optical networks [24], however, this is a specific solution for short to mid-term fluctuations in IPoWDM

networks.

Once the traffic model is fixed, algorithms are needed to place lightpaths into the network, to carry the required traffic between any given source-destination pairs. Since the advent of flex-grid networking, Routing and Spectrum Assignment (RSA) algorithms have given way to Routing, Configuration Selection, and Spectrum Assignment (RCSA) algorithms. Further explanation of the differences between RSA and RCSA algorithms follows in Section 3.1.

Several works have looked into RCSA from a flex-grid network planning viewpoint. Broadly, there are three mathematical tools available for solving this task. The first solution relies on modelling the RCSA problem mathematically, using integer linear programming (ILP) [15, 25]. Although it is possible to model and add additional objectives or constraints, the computational complexity is large due to a broad solution space. Also, such a solution is difficult to scale for large network studies, due to the lightpath continuity and contiguity constraints for all the demands. A second solution emergent in recent years is to use machine learning techniques such as deep learning or reinforcement learning [26, 27]. The motivation to use machine learning for this task is to take advantage of its highly efficient algorithmic mappings and find a solution in polynomial time, which might not be possible for ILP-based algorithms. However, it is challenging to train a model or build an agent which can learn many parameters together. Such models also run the risk of acquiring high dimensions, thereby making it difficult for the agent to infer a good policy.

As an attempt to procure a solution in polynomial time, a combinatorial heuristic-based approach can also be taken. This involves splitting the RCSA problem into independent smaller modules and solving them separately [28]. Without the guarantee of optimality, such algorithms can provide quick solutions, thereby allowing planners to try multiple scenarios.

Pure heuristics-based RCSA algorithms like Maximum Capacity Algorithm [29] and HeCSON [30] are indeed simpler to implement. However, these models are unable to optimize the candidate lightpaths according to the demand in a multi-period planning scenario, which leads to spectrum blocking for future traffic

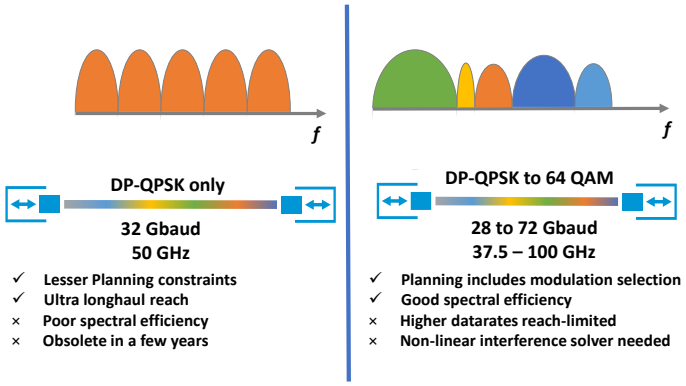

Figure 2: Fixed-grid versus flex-grid transceivers

increases. To emphasize maximizing the per-lightpath capacity, while reducing the spectral usage for multi-period planning, a multi-objective combinatorial heuristic-based solution was introduced [31]. With the ability to achieve a near-optimal solution to an NP-hard problem in polynomial time, this approach is used as a baseline for conducting network planning studies in our work.

A recent work [32] also provides upgrade strategies for operators to move to L and S-band transmission, thereby providing a combinatorial heuristic-based planning tool to undertake RCSA. However, results are shown for only a single network and the methodology cannot be generalized without further results.

Therefore, our work undertakes a long-haul network operator-centric planning study to increase the offered traffic in single-mode fiber core network deployments. To this end, we extend our previous work [30, 33], by firstly introducing a stochastic traffic model, taking into account new population and graph metrics. Secondly, we introduce a combinatorial heuristics-based multi-period RCSA planning and compare two distinct multi-band deployment methods. Finally, we evaluate the network deployment CAPEX using a simple cost model to compare the costs of Flex-BVT and multi-haul CFP2-DCO deployments.

3. System Design Considerations for Network Upgrade

In this section, we elaborate on two methods that core network operators can use to increase the capacity of their network. In the first method, upgrading terminal equipment, without upgrading the OLS is discussed. In the second method, a migration towards a C+L+S-Band OLS is discussed. We highlight both the benefits and shortcomings of such upgrades.

3.1. Flex-BVT vs Transparent IPoWDM deployment

As introduced in Section 1.1, Flex-BVT aggregates 10, 25, 40, 100, 200, and 400 GbE client interfaces into a single network side optical signal which can be set to different modulation formats and baud rates, based on the traffic demand requirements. In our work, we define such an optical signal, which can be launched into the OLS, as a lightpath. Traditionally, fixed-grid systems offer 32 GBaud QPSK lightpaths, capable of 100 Gbps capacity. With a spectral efficiency of 2 bits/s/Hz, this solution can be now replaced by Flex-BVTs, which can offer up to 6 bits/s/Hz of spectral efficiency, provided the optical transmission suffices.

If operators choose a Flex-BVT-based network upgrade, they need to apply newer methods for network planning and deployment. Specifically, the RSA problem for placing candidate lightpaths in the network transcends to an RCSA problem. In RCSA, each Flex-BVT configuration can be defined as a combination of modulation format, baud rate, and channel launch power, such that the lightpath's generalized signal-to-noise ratio (GSNR) meets the minimum required SNR of the transceiver. In our work, we follow the definition of GSNR from [7, 20, 21, 34], where the GSNR of a lightpath can be defined as the ratio of the channel launch power to the sum of the linear and non-linear interference (NLI). The linear noise is mainly the Amplified Spontaneous Emission (ASE) noise from the in-line amplifiers along the route of the lightpath, whereas the non-linear interference originates from the inter-channel and inter-symbol interference of the neighbouring lightpaths along the lightpath's route.

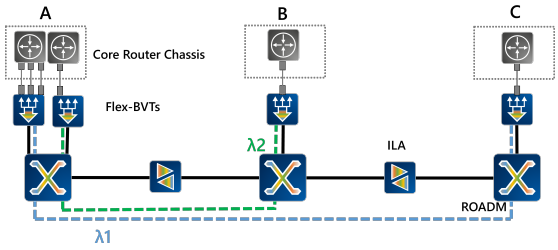

(a) Flex-BVT-based DWDM and IP layer network architecture

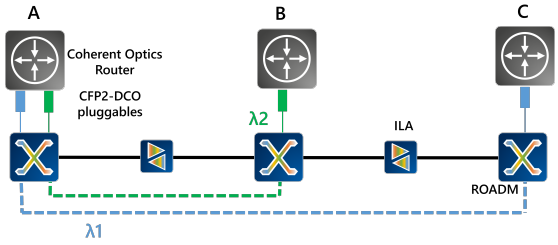

(b) CFP2-DCO-based transparent IPoWDM architecture

Figure 3: Flex-BVT versus CFP2-DCO deployment for a simple 3 node 2 lightpath link.

Moreover, since the spectrum is not evenly spaced, lightpaths need to be allocated in a manner that reduces the overall NLI noise for the whole system. This results in additional allocation constraints since the placement of a candidate lightpath should not hamper any of the currently installed lightpaths. This is discussed in detail in Section 5.

As shown in Fig. 3a, the advantage of the Flex-BVT deployment strategy is that the operator can re-use most of the Layer 3 core routers, since the BVTs act as an intermediary between the core routers and the OLS. Further, the network operator is no longer restricted to choosing coherent optics-based routers, leading to wider flexibility in the choice of routers.

In Fig. 3b, a multi-haul CFP2-DCO-based transparent IPoWDM architecture achieves data rates up to 400 Gbps by eliminating the optical terminal and using coherent optics enabled core routers which have CFP2-DCO cages. Each of these CFP2-DCO pluggables can be tuned to a specific central channel

frequency on the C-Band and launched directly into the OLS. The advantage of such a solution is that the network operator does not need to invest in additional optical terminals, since the Optical-Electrical-Optical (O-E-O) conversion happens on board the pluggable, while the core router takes care of the electrical grooming of client interfaces. The disadvantage, however, is that the network operator must deploy expensive core routers which can provide enough power and backplane switching capacity to support such pluggables.

Traditionally, an IPoWDM deployment consists of network deployments that use QSFP-DD-based pluggables. These pluggables have the capability of achieving up to 400 Gbps and can be integrated into QSFP-DD cages on core IP routers. However, due to the smaller footprint and reach limitations of these pluggables, they are restricted to metro and data-center applications. A long-haul network with QSFP-DD pluggables can be realized by using an opaque deployment, which has several disadvantages, both from a techno-economic and operations perspective [17]. On the other hand, multi-haul CFP2-DCO pluggables are a more suitable option to realize transparent IPoWDM networks, since they provide similar reach as compared to a Flex-BVT, but are less expensive. Therefore, it is pertinent that the suitable IPoWDM pluggable is chosen, based on the type of networks and requirements of the operators [18].

While Flex-BVT-based and CFP2-DCO-based transparent IPoWDM architectures have their advantages and disadvantages, network operators must evaluate both scenarios and invest accordingly. Hence, we consider this decision as the first step in undertaking network upgrades to tackle rising traffic demands.

3.2. Migration towards multi-band planning

Eventually, the addition of more Flex-BVTs or CFP2-DCO pluggables will lead to C-Band (191.0 - 196.0 THz) saturation. This means that network operators have to aim for OLS upgrades by revisiting each node and amplifier hut location to add new equipment for multi-band amplification. In this work, we consider the deployment of parallel amplification using a band splitter and combiner.The three transmission bands considered have the frequency band lim-

its as shown in Table 2 and are comparable to the band limits defined in the state-of-the-art [32, 34].

Band	Frequency Range (THz)	Frequency Slots @ 12.5 GHz
C-Band	191-196	400
L-Band	185-190	400
S-Band	197-202	400

Table 2: Frequency band limits and number of frequency slots for C, L, and S bands [34].

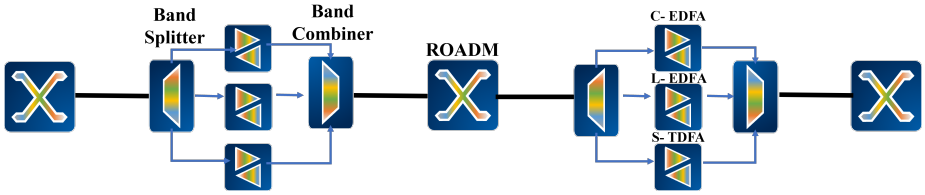

Figure 4: Example of Multiband OLS transmission for a 3 node 2 link network

Several physical layer considerations need to be made to plan lightpath deployment on L and S bands. Firstly, assuming standard single-mode fibers, the attenuation coefficient (dB/km) is different for each band of operation. Secondly, as shown in Fig. 4, C-Band and L-Band can be amplified by different EDFAs and the S-Band can be amplified by a TDFA. Although the EDFAs are different, both C- and L-Band EDFAs can be assumed to have similar noise figures. For the S-Band TDFA, a higher noise figure is assumed [34]. Due to the varying attenuation co-efficient noise figure of amplifiers, the ASE noise is different for the three bands. Inter-channel stimulated Raman scattering (ISRS) is an important phenomenon observed in ultra-wideband optical systems. ISRS is defined as the interaction between photons and vibrations of silica molecules which results in a power transfer from higher frequency channels to lower frequency channels [35]. Hence, to consider this as a part of NLI noise in our studies, we use a modulation format-dependent closed-form approximation of the ISRS-GN model, introduced by Semrau et. al [36]. Finally, launch power optimization is a crucial aspect not only of maximizing the optical reach but

also of accurately modelling the ASE and NLI noise. Several works use the LOGO optimization strategy to find a per-band flat launch power [7, 21]. In [20], the authors also provide an optimized launch power offset value (in dBm) and a launch power tilt value (dB/THz), which we use in our calculations.

Therefore, after assimilating all the physical layer considerations, we now proceed further with the network planning aspects and focus on our two major contributions, namely, a realistic traffic generator model, and a combinatorial heuristics-based RCSA algorithm which can be applied for a multi-period network planning scenario.

4. Traffic Generator

As discussed in Section 2, there is both a lack of realistic long-haul network traffic profiles, as well as traffic models, which can be used to generate traffic between a given source and destination in a network. Long-haul traffic models based on human population density and telephony volume are obsolete, since most of the long-haul traffic is exchanged between core datacenters (DCs) and internet exchange points (IXPs). In recent times, private datacenter interconnect requests have been identified as the biggest traffic drivers [37]. To circumvent this lack of information, capacity planning studies use generalized network metrics such as lightpath arrival and holding time [14]. However, these metrics do not sufficiently mirror the on-ground reality of deployed networks. Long-haul transparent lightpaths usually have extremely long holding times, and are not removed from the system, once placed. Also, the demand arrival rate is fixed into planning periods, like years or quarters. Therefore, to simulate expected traffic, we propose a simple traffic generator model, which is based on the number of core DCs and IXPs present in a given network location, as well as some graph metrics. The proposed traffic model can be divided into two broad parts, namely, *initial traffic estimate*, and *multi-period traffic increase*. These parts are now discussed in detail.

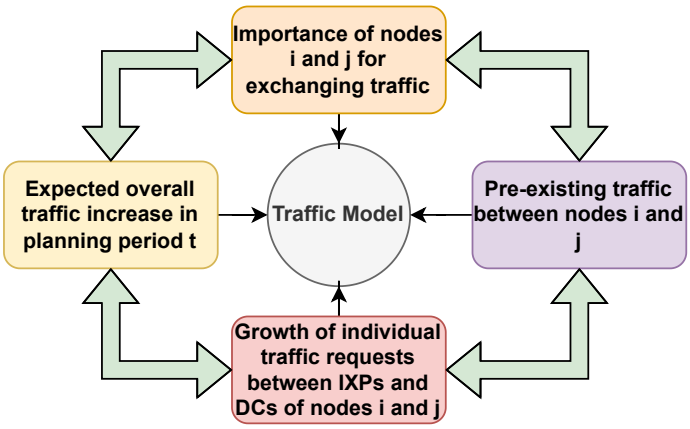

Figure 5: Factors influencing traffic generated between source i and destination j in planning period t

4.1. Initial Traffic Estimate

Let us define the optical network topology as a graph $\mathcal{G}(\mathcal{V}, \mathcal{E}, \mathcal{D})$. $\mathcal{V}$ is the set of Points-of-Presence (PoPs) in the network, where traffic can be added or dropped. $\mathcal{E}$ is the set of links, where each link is defined as a collection of standard single-mode fiber spans in the ground, connecting any two nodes belonging to $\mathcal{V}$. $\mathcal{D}$ is defined as the set of demands in the network. Each node in the network has a demand associated with every other node in the network. Further, each node κ has an associated metric on the number of co-located DCs (DC_κ) and IXPs (IXP_κ). For the network, we also define $\bar{N}$ as the average node degree of the network, and for each demand $d_{i,j} \in \mathcal{D}$, $N = n_i + n_j$ represents the combined node degree of the source node i and destination node j.

To derive a model for the initial traffic estimate, we first assume a hierarchical structure of the co-located DCs and IXPs at each node location. Here, two important assumptions are made, namely, *(i)* intra-node traffic (i.e. DC to IXP within the same location) is not accounted for in a long-haul traffic model, and *(ii)* inter-node traffic consists of only DC-DC and IXP-IXP interconnects. This modelling helps us reduce long-haul transparent network demands and allows

intra-node aggregation networks to serve the inter-node DC-IXP and IXP-DC traffic.

Firstly, we define the number of IXP and DC connections to be established between source node i and destination node j in the network as,

$$\Delta_{i,j} = IXP_i \cdot IXP_j + DC_i \cdot DC_j \tag{1}$$

where IXP_k and DC_k are the number of IXPs and DCs in a given node $k \in \mathcal{V}$. This ensures we cover all the IXP-IXP and DC-DC connections between the networks. However, there is also the need to remove any DC-IXP interconnects in line with the second assumption. Therefore the number of connections to be established can be modified as

$$\Delta_{i,j} = IXP_i \cdot IXP_j + DC_i \cdot DC_j - DC_i \cdot IXP_j - DC_j \cdot IXP_i \tag{2}$$

Simplifying the equation, we obtain:

$$\Delta_{i,j} = |DC_i - IXP_i| \cdot |DC_j - IXP_j| \tag{3}$$

From the combined node degree N, one egress link on the source node and one ingress link on the destination node are used for the traffic flow. Therefore, we multiply Eq. 3 with a combination equation of choosing two degrees from N. For sparsely connected nodes, the combination equation is replaced with the combined node degree. Hence, the total flow is defined as

$$\theta_{i,j} = \begin{cases} \binom{N}{2} \cdot \Delta_{i,j} & \text{if } N > 2 \cdot \bar{N} \\ N \cdot \Delta_{i,j} & otherwise \end{cases} \tag{4}$$

To estimate the initial traffic at planning period $t = 0$ between source i and destination j, the number of flows $\theta_{i,j}$ need to be multiplied by the per-interconnect demand in Gigabits per second (Gbps). For this, we chose two interconnect demands at the beginning of the planning period, namely, $\alpha_1 = 10\ Gbps$ and $\alpha_2 = 7.5\ Gbps$. α_1 is assigned for flows between densely connected nodes, whereas α_2 is assigned for flows between sparsely connected nodes. Moreover, a constant β is set to 100 Gbps, which is assumed to be the minimum

demand request between the source and destination, so that if $\Delta_{i,j}$ becomes nullified, there should be at least a 100 Gbps demand available. Therefore, the initial traffic at $t = 0$ for a demand $d_{i,j} \in \mathcal{D}$ is given as:

$$\tau(i,j,0)[Gbps] = \begin{cases} \alpha_1 \cdot \theta_{i,j} + \beta & \text{if } N > 2 \cdot \bar{N} \\ \alpha_2 \cdot \theta_{i,j} + \beta & otherwise \end{cases} \tag{5}$$

4.2. Multi-period Traffic Increase

In our previous work [30], once the initial traffic for each demand was calculated, an aggregated traffic growth, normally distributed around a mean of 25% annually was employed. While simple, this method does not cater to the uncertainty of unbalanced scaling of traffic. To this end, in this work, we add a new traffic model which decouples the traffic growth from the initial traffic demand. Let us begin by defining the variables of this traffic model.

Since the yearly traffic growth rates of around 25% are a common phenomenon, we define the overall expected traffic increase δ_t in a given planning period t as,

$$\delta_t = \tau_{t-1} \cdot \mathcal{X}_\tau \tag{6}$$

where τ_{t-1} is the aggregate traffic distribution of the previous planning period and $\mathcal{X}_\tau \leftarrow \mathcal{N}(\mu_\tau, \sigma_\tau^2)$ is random variable drawn from a normal distribution with μ_τ set to 0.25 and σ_τ set to 0.1. The mean of 25% growth is assumed from global network traffic growth predictions [38], whereas the deviation is extrapolated using the measurements reported by Soule *et. al* [39].

Further, we define the increase in traffic of individual demands, acknowledging the non-uniform traffic growth for each node in the network. For this, we first define a node-importance metric $\mathcal{I}_v$ for a node $v \in \mathcal{V}$ as,

$$\mathcal{I}_v = \Lambda_v + 100 \cdot (IXP_v + DC_v) \cdot \mathcal{C}_v \tag{7}$$

where Λ_v and $\mathcal{C}_v$ is the eigenvector centrality and the closeness centrality metric of the node $v \in \mathcal{V}$ in the graph $\mathcal{G}(\mathcal{V}, \mathcal{E}, \mathcal{D})$ respectively. IXP_v and DC_v are the number of co-located IXPs and DCs at node v.

From Eq. 7, it can be inferred that nodes that are better connected and have a higher number of IXPs or DCs are the ones that will have higher importance. Once the importance of each node is calculated, we find the normalized value of this importance metric $\mathcal{I}_{v,norm}$, such that the value for each node lies between 0 and 1, and the sum of all the normalized importance metric is 1.

$$\mathcal{I}_{v,norm} = \frac{\mathcal{I}_v}{\sum_{\nu \in \mathcal{V}} \mathcal{I}_\nu} \tag{8}$$

Fig. 6 shows as an example the normalized importance metric of each node in a 17-node German network. Nodes like Frankfurt have higher importance since they are both well connected and have a higher number of DCs and IXPs, whereas nodes like Munich, although having more number of DCs and IXPs, lie lower in the importance list, due to their location in the graph.

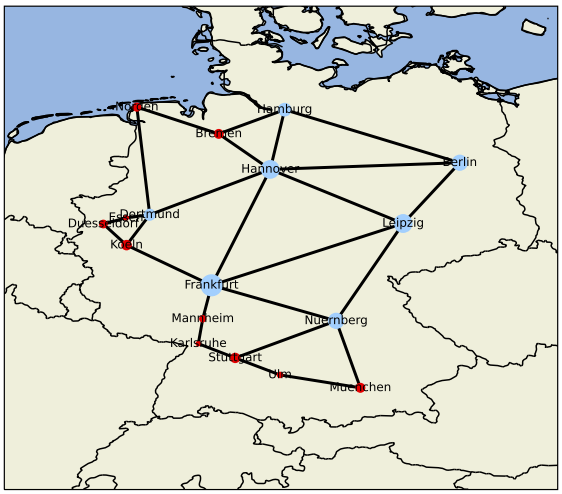

Figure 6: German network, with node size proportional to the normalized node importance metric. Blue-colored nodes have a higher likelihood of exchanging traffic.

Since each demand $d \in \mathcal{D}$ has a source and a destination node $(i, j) \in \mathcal{V}$, a joint probability density function to select a demand using the normalized importance metric of each node can be calculated as,

$$\mathcal{F}_d(i,j) = \frac{\mathcal{I}_i \cdot \mathcal{I}_j}{\sum_{(a,b) \in \mathcal{V}} (\mathcal{I}_a \cdot \mathcal{I}_b)} \tag{9}$$

Therefore using Eq. 9, we draw a demand $d \leftarrow \mathcal{F}_d(i,j)$ and calculate the additional traffic request generated by it in the planning period as,

$$\delta(i,j,t)[Gbps] = D_{DC,t} \cdot (DC_{i,j}) \cdot e^{\mathcal{X}_{DC} \cdot t} + D_{IXP,t} \cdot (IXP_{i,j}) \cdot e^{\mathcal{X}_{IXP} \cdot t} \quad (10)$$

Here, $D_{DC,t}$ and $D_{IXP,t}$ are defined as the inter-DC and inter-IXP interconnection request at a given planning period t, and take the following values,

$$(D_{DC,t}, D_{IXP,t})[Gbps] = \begin{cases} (10,40) & if\ t \leq 3 \\ (40,100) & if\ 4 \leq t \leq 7 \\ (100,400) & otherwise \end{cases} \quad (11)$$

$DC_{i,j} = DC_i + DC_j$, $IXP_{i,j} = IXP_i + IXP_j$, are the sum of the number of DCs and IXPs at the source and destination. $\mathcal{X}_{IXP} \leftarrow \mathcal{N}(\mu_{IXP}, \sigma^2_{IXP})$, and $\mathcal{X}_{DC} \leftarrow \mathcal{N}(\mu_{DC}, \sigma^2_{DC})$ are the IXP and DC growth rates drawn from their respective random normal distributions.

10, 40, 100, and 400 refer to the additional traffic request base values in Gbps generated between each DC and IXP at the source and destination. These values are increased every 4 planning periods, assuming that there will be increasing technology adoption on higher layers, which would lead to interconnect traffic demand increase at the OLS side. Moreover, the demand request also depends on an exponential increase from the base values of DC and IXP interconnects. Specifically, these growth rates are drawn from a random variable with a Gaussian distribution, whose mean values are 0.35, 0.25 and standard deviation values are 0.1, 0.05 respectively [38, 39].

This process continues till the sum of all additional traffic from all drawn demands reaches the aggregate additional traffic δ_t as defined in Eq. 6. Therefore, using this method, we can achieve a skewed demand distribution, with more traffic flowing between nodes of importance. This is especially helpful in multi-period network planning studies, where the demands need to not only increase, but also introduce stochastic events in the simulation.

5. RCSA Algorithm

RCSA algorithms for optical networks not only serve as a tool to plan new services into the networks, but also conduct forward-looking strategic studies, and provide stakeholders a cost and effort estimate. Not only this, RCSA algorithms are used by Path Computation Elements (PCE) in network orchestrators and software-defined networking (SDN) controllers for in-operation service planning and deployment.

As discussed in Section 2, several solutions for the RCSA problem exist in the literature. However, with changes in network studies and input parameters, there is a lack of generality in many RCSA algorithms. Having evaluated a heuristic method, and a pure ILP-based approach, we choose the middle ground with a combinatorial heuristics-based approach. Our work extends [30, 31] by utilizing a *'divide and conquer'* policy by splitting the routing, configuration selection, an spectrum allocation into independent sub-problems. This allows us the flexibility to choose either a heuristic or an ILP for each of the sub-problem. For the routing and configuration pre-selection, we use a heuristic approach, whereas, for the candidate lightpath configuration assignment, we design a multi-objective ILP. Finally, for spectrum allocation, we use the first-fit allocation strategy. In the subsequent sections, we discuss in detail the routing and pre-selection algorithm, the ILP for candidate lightpath selection, and finally the multi-period RCSA algorithm which combines all parts into a multi-period planning problem.

5.1. Routing and Configuration Pre-Selection

Before the periodical planning of lightpaths for the given traffic request begins, we undertake two major steps, namely, routing of source-destination pairs, and a pre-selection of candidate lightpath configurations, based on the optical performance of the given Flex-BVT/CFP2-DCO in all the bands of operation. Algorithm 1 gives an overview of this process.

For the routing, we assume a $k = 3$ Dijkstra's shortest path non-disjoint routing for each source-destination pair in the demand matrix $\mathcal{D}$. Since we are

Algorithm 1: Routing and Configuration pre-selection algorithm

function RouteAndPreselect ($\mathcal{G}(\mathcal{V}, \mathcal{E}, \mathcal{D})$, $\mathcal{C}$);

Input : Network topology $\mathcal{G}(\mathcal{V}, \mathcal{E}, \mathcal{D})$ and Flex-BVT/CFP2-DCO configuration list $\mathcal{C}$

Output: Ordered list of routed demands $\mathcal{D}$ and possible configurations for all demands $\mathcal{C}_{\mathcal{D}}$

for $d \in \mathcal{D}$ **do**
    $SP_d \leftarrow$ Yen's $k = 3$ shortest paths of d;
    $Hops_d \leftarrow$ num hops of $SP_d[0]$;
end
Order $d \in \mathcal{D}$ longest to shortest SP_d then highest to lowest $Hops_d$;
for $d \in \mathcal{D}$ **do**
    for $k \leftarrow 0$ *to* 2 **do**
        for $c \in \mathcal{C}$ **do**
            Place set of lightpaths $L_{d,k,c}$ with config c on all freq slots of links $e \in SP_d$;
            Calculate $GSNR_{d,k,c,l} \forall\ l \in L_{d,k,c}$ [36] ;
            $GSNR_{d,k,c} \leftarrow \min(GSNR_{d,k,c,l})$;
            if $GSNR_{d,k,c} \geq minSNR_c$ **then**
                $c \rightarrow \mathcal{C}_{d,k}$;
            end
            Remove $L_{d,k,c}$ from all freq slots ;
        end
        $\mathcal{C}_{d,k} \rightarrow \mathcal{C}_d$;
    end
    $\mathcal{C}_d \rightarrow \mathcal{C}_{\mathcal{D}}$;
end
return $\mathcal{D}$, $\mathcal{C}_{\mathcal{D}}$

dealing with long-haul networks, we observed that the path diversity increases drastically for higher values of k, thereby leading to higher delays and lower data rates per transparent lightpath. Once the source-destination pairs are assigned their routes, they are ordered according to their first shortest path lengths, with the source-destination pair having the longest route being assigned the highest priority. Then, source-destination pairs with similar path lengths ($\leq 100km$) are ordered according to the number of hops, with the pairs having a higher number of hops being assigned a higher priority. This is done to introduce fairness in the simulation so that the pairs using more links are not blocked later by pairs using fewer links but more spectral resources.

Next, using our previously proposed heuristic for configuration selection, 'HeCSON', we select candidate Flex-BVT/CFP2-DCO configurations for each source-destination pair in the network [30]. For each possible configuration, HeCSON simulates a fully-loaded homogeneous channel and finds the worst-case channel GSNR using the modulation format dependent ISRS GN model to calculate the NLI noise term [36]. The ISRS GN model is used here, because of its capabilities to estimate NLI noise for central channel frequencies in a multi-band scenario. To ensure that the NLI noise in the L and S bands is not underestimated, we also add additional GSNR margins to calculated GSNR, as given in [40]. For each routed demand, the configurations whose worst-case calculated GSNR is lesser than the minimum receiver sensitivity SNR are removed from the list of possible configurations. After this, we need to find the candidate lightpaths which may satisfy the traffic requirement for each of the demands.

5.2. Selecting Candidate Flex-BVT/CFP2-DCO configurations

Once the paths and configurations of all source-destination pairs and the traffic matrix for the current planning period τ_t (ref. Eq. 10) are calculated, for each demand, we need to assign suitable configurations for each network terminal card, such that the traffic demand between each source-destination pairs can be satisfied with minimum equipment. Here, we extend the multi-

objective lightpath 'selection' ILP definition from [30, 31].

Let us consider a demand $d(i,j) \in \mathcal{D}$ in planning period t, with additional requested traffic $\delta(i,j,t) \in \tau_t$ (ref. Eq. 10). It may be the case that some of the additional requested traffic may already be satisfied by some in-operation lightpaths. Therefore, the traffic to be met between source i and destination j of demand d at a given time t is defined as $\rho(i,j,t) = \tau(i,j,t-1) + \delta(i,j,t) - \sum_{\forall l \in \widetilde{L_d}} DR_l$, where $\tau(i,j,t-1)$ is the total requested traffic up to the previous planning period for demand d, and $\sum_{\forall l \in \widetilde{L_d}} DR_l$ is the sum of the data rates DR_l of all the in-operation lightpaths $\widetilde{L_d}$ belonging to demand d.

Using the above definitions, the selection of candidate lightpaths from the demand's possible configurations $\mathcal{C}_d \in \mathcal{C}_\mathcal{D}$ is defined as,

$$\text{Minimize} \sum_{c \in C_d} \sum_{p \in SP_d} x_{c,p}, \text{Maximize} \sum_{c \in C_d} \sum_{p \in SP_d} \big(x_{c,p} \times R_c\big), \tag{12}$$

$$\text{such that } : \rho(i,j,t) \leq \sum_{c \in C_d} \sum_{p \in KSP_d} x_{c,p} \times R_c \leq \rho(i,j,t) + \eta, \tag{13}$$

$$\sum_{c \in C_d} x_{c,p} \times BW_c \leq \widetilde{BW}_p, \forall p \in SP_d, \tag{14}$$

$$\text{integer variables } x_{c,p} \geq 0, \forall c \in C_d, \forall p \in SP_d.$$

In Eq. 12, we define a multi-objective integer linear objective function, which minimizes the number of candidate lightpaths (integer variable $x_{c,p}$) while maximizing the datarate R_c of each of the candidate lightpaths associated with configuration $c \in C_d$ along path $p \in SP_d$.

This objective function is constrained by Eq. 13, known as the data rate constraint. η is a constant which limits the overprovisioning of the datarate, avoiding greedy usage of spectral resources.

In Eq. 14, we introduce a bandwidth constraint for each path $p \in SP_d$, such that the total bandwidth of all candidate lightpaths on path $p \in SP_d$ shall not exceed the maximum available contiguous bandwidth on the path p, denoted by $\widetilde{BW}_p$.

Using Eq. 12-14 allows an optimal selection of candidate lightpaths which

can be then placed onto the spectrum Once the lightpaths are placed and the traffic is satisfied for demand, we move to the next demand, and continue this operation till all the demands in the given planning period are satisfied.

5.3. Multi-period RCSA algorithm

In a multi-period planning scenario, the heuristics and ILPs previously discussed in this section are used to place lightpaths into the network, to cope with the per-period increase in data rate demands between any given source i and destination j in the network.

Algorithm 2 provides an overview of the described RCSA algorithm in a multi-period scenario. As a pre-requisite, the candidate paths of demands $\mathcal{D}$ and their corresponding candidate configurations $\mathcal{C}_{\mathcal{D}}$ should already be pre-calculated using the routing and configuration pre-selection algorithm (ref. Alg. 1). For each planning period $t \in \mathcal{T}$, we iterate over each demand $d \in \mathcal{D}$ to find the source i and destination j belonging to it. Once the additional requested traffic $\delta(i, j, t)$ is calculated, the in-operation lightpaths $L_d \in \mathcal{L}$ need to be upgraded. The upgrade occurs without using additional spectral resources, and without changing the center channel frequency of each in-operation lightpath. The upgraded in-operation lightpaths for the demand d are denoted as $\widetilde{L_d}$. Further details on the lightpath upgrade heuristic are available in our previous work [30].

Using the data rate of the upgraded lightpaths for demand d, $\rho(i, j, t)$ is calculated as described in the previous section. If the upgraded in-operation lightpaths are unable to satisfy the additional requested traffic (i.e. $\rho(i, j, t) > 0$), we invoke Eqs. 12-14 to find the optimal candidate lightpaths for the demand. The candidate lightpaths $L_{d,t}$ are added to the spectral slots available on the links in a first-fit fashion. The newly placed lightpaths are denoted as $L"_{d,t}$. In case some lightpaths cannot be placed, the re-routing algorithm is invoked [31]. Since the in-operation lightpaths change their bandwidths or central channel frequencies, the GSNR for all the in-operation lightpaths sharing the same links

Algorithm 2: Multi-period RCSA Algorithm

function MultiperiodRCSA ($\mathcal{G}(\mathcal{V},\mathcal{E},\mathcal{D})$, $\mathcal{C}, T$);

Input : Network topology $\mathcal{G}(\mathcal{V},\mathcal{E},\mathcal{D})$, transceiver configuration list $\mathcal{C}$, total planning period T

Output: List of placed lightpaths $\mathcal{L}$, yearly underprovisioning $\mathcal{U}$

$\mathcal{D}, \mathcal{C}_{\mathcal{D}} \leftarrow$ RouteAndPreselect($\mathcal{G}(\mathcal{V},\mathcal{E},\mathcal{D})$, $\mathcal{C}$) [Alg. 1]

for $t \in \mathcal{T}$ **do**

  for $d \in \mathcal{D}$ **do**

    $(i,j) \leftarrow d$;

    $\delta(i,j,t) \leftarrow \tau_t(d)$;

    $\widetilde{L_d} \leftarrow$ UpgradeLP($L_d \in \mathcal{L}$) [30];

    Recalculate GSNR for all placed lightpaths sharing the same links as $\widetilde{L_d}$;

    Calculate $\rho(i,j,t)$;

    if $\rho(i,j,t) \geq 0$ **then**

      $L_{d,t} \leftarrow$Eqs. 12-14;

    else

      continue;

    end

    $L"_{d,t} \leftarrow$ First-Fit($L_{d,t}$);

    if $\rho(i,j,t) \geq \sum L"_{d,t}$ **then**

      $L"_{d,t} \leftarrow$ Reroute(d,$\mathcal{L}$,t) [31]

    end

    Recalculate GSNR for all placed lightpaths sharing the same links as $L"_{d,t}$;

    $\rho(i,j,t) \leftarrow \rho(i,j,t) - \sum_{\forall l \in L"_{d,t}} DR_l$;

    $L"_{d,t} \rightarrow \mathcal{L}$;

    if $\rho(i,j,t) \geq 0$ **then**

      Increase underprovisioning $\mathcal{U}$ using Eq. 15

    end

  end

end

return $\mathcal{L}$, $\mathcal{U}$

as $L"_{d,t}$ needs to be re-calculated. The remaining traffic for demand d, given by $\rho i, j, t$ is updated by subtracting the data rate of the placed lightpath $L"_{d,t}$. Finally, in case there is traffic remaining that could not be assigned to a lighpath, the underprovisioning percentage $\mathcal{U}$ is increased using Eq. 15.

To fairly measure the number of demands which could not meet the requested traffic, we introduced "underprovisioning" in our previous work [33]. For a given planning period t, underprovisioning is defined as the ratio of the sum of all demand data rates which could not be provisioned in the network to the overall requested aggregate traffic. In our work, underprovisioning UP_t is represented as a percentage, and can be calculated as follows:

$$UP_t = \frac{\sum_{\forall \widetilde{d} \in \widetilde{D}_t} (DR_{\widetilde{d}} - \sum_{\forall l \in LP_{\widetilde{d}}} DR_l)}{\sum_{\forall d \in \mathcal{D}_t} DR_d} \cdot 100\ \% \tag{15}$$

where $\widetilde{D}_t$ is the set of demands in planning period t which could not be satisfied by the placement of in-operation lightpaths $l \in LP_{\widetilde{d}}$. $\mathcal{D}_t$ is the set of all demands in the planning period t.

6. Network Studies and Techno-economic Analysis

In this section, we undertake a multi-period network planning study using the RCSA algorithm discussed in Section 5. Here, we first describe the networks under study and the simulation setup. Then, we compare network metrics like throughput, placed lightpaths, and underprovisioning, of a multi-band Flex-BVT deployment, with a multi-band transparent IPoWDM deployment. For both terminal deployment strategies, we also compare when must an operator plan for lighting the S and L bands. Finally, we introduce a multi-layer techno-economic cost model and find the total cost of ownership (TCO) of both a Flex-BVT and a CFP2-DCO-based multi-band architecture.

To compare the results of a long-term network deployment on multiple topologies, we use three European national network topologies, namely, Germany, Spain, and Sweden. These networks have been retrieved from the Inter-

Network	**Topology Parameters**			**Lightpath Lengths [km]**		
	Nodes	Links	Demands	Min	Avg.	Max
Germany	17	26	121	34.50	558.47	982.00
Spain	16	27	135	112.79	871.81	1598.67
Sweden	25	29	286	20.00	1066.18	3533.34

Table 3: Topology and route statistics for European core networks under study [41].

net Topology Zoo [42] and have been converted into a physical layer fiber and span topology, which is available as an open-source dataset [41].

The network topologies are shown in Fig. 7, and from a graph perspective, the three networks are topologically different. As reported in Table 3, Germany is a well-connected mesh network with 17 nodes and 26 links and has an average lightpath length of around 550 km. Spain is a 16-node 27-link topology in a star-shaped topology, with Madrid serving as the central node. The longest lightpath

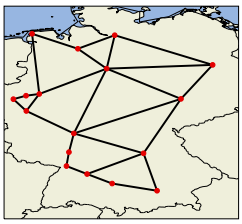

(a) Germany

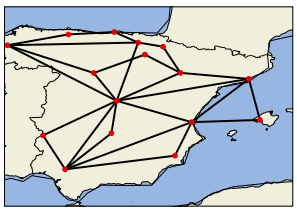

(b) Spain

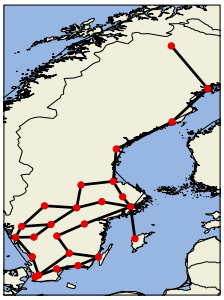

(c) Sweden

Figure 7: European Core Networks under study. We assume a single SSMF fiber pair between any two nodes.

is almost 1600 km. Finally, in Sweden, many nodes are connected with a single point-to-point link, with the longest transparent lightpath achieving more than 3500 km. Looking at the statistics of lightpath lengths, it is clear that both Flex-BVTs and CFP2-DCO-based architectures can operate with at least a 32 GBaud QPSK configuration on the longest route on each network.

In this work, we design a multi-period network planning study, which is run for 10 planning periods on the three mentioned topologies. The fiber topology of these networks assumes a single SSMF fiber pair between the two nodes. For multi-band transmission, we consider different values for fiber attenuation, amplifier noise, launch power, and minimum required GSNR for each band, taking values from [20]. In these studies, we utilize the RCSA algorithm discussed in Section 5, and simulate two deployment scenarios, namely Flex-BVT, and transparent IPoWDM. The simulation software is implemented in *Java*, and runs on a machine with a 12th Generation Intel® Core™ i7-12700K processor, with 32GB RAM. To ensure a fair comparison of the two scenarios, we invoke two parallel runs of the multi-period RCSA algorithms, which are fed the per-period demand from the same instance of the traffic model discussed in Section 4. For each network, we run the multi-period planning 1000 times to generate a confidence distribution over the results.

6.1. Traffic Model Validation

Since our proposed traffic model is an important input to the network planning study, we need to compare and validate the model with the traditional gravity-based traffic model [43], and with the CISCO VNI report on traffic growth for three network topologies under test.

The gravity model defines the traffic $t_{s,d}$ flowing between a source s and destination d in a long-haul core network as $t_{s,d} = k \cdot \frac{P_s \cdot P_d}{L^{\phi}}$, where P_s and P_d are the population metric at source and destination and L is the distance between them. k and ϕ are the scaling factors for the traffic. For this comparison, we assume the population metric P_s and P_d to be the sum of IXPs and DCs at the

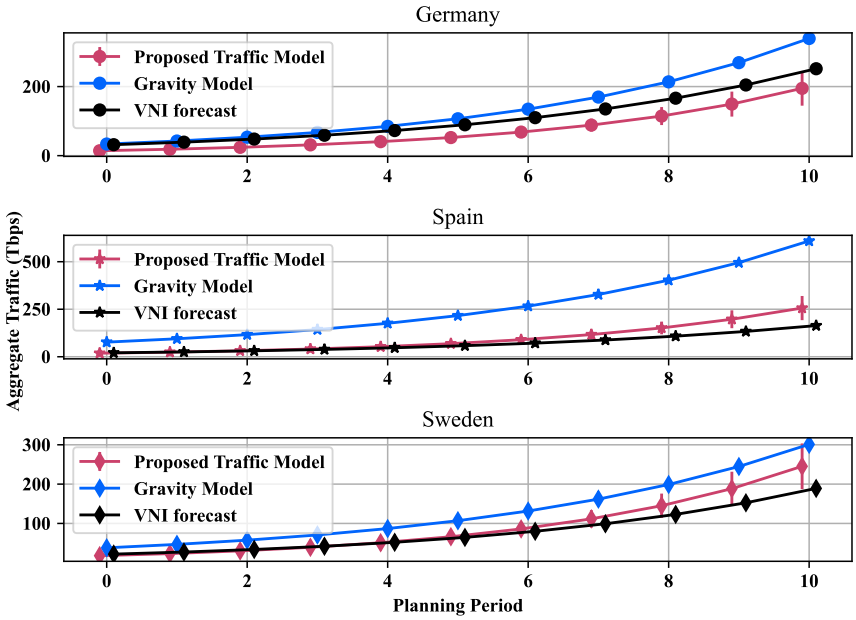

Figure 8: Traffic Model comparison for the German, Spanish, and Swedish core networks.

source and destination respectively. ϕ is set to 2, assuming two different types of traffic are being carried. Scaling factor k varies according to the network and is chosen using trial and error to achieve similar order of magnitude as the initial aggregate traffic mentioned in the 2021 CISCO VNI forecast highlights [38]. Since this forecast provides traffic statistics for the whole country, we make a simple assumption that the market penetration is uniformly distributed amongst the long-haul network operators in the country. The traffic increase rates for the gravity model and the VNI forecast are the same as the Compounded Annual Growth Rate (CAGR) mentioned for each of the countries in the CISCO VNI forecast. The discussed parameters are assimilated into Table 4.

As seen in Fig. 8, the proposed traffic model follows the forecasted traffic growth closely. The gravity model, on the other hand, tends to deviate from the forecasted growth, despite having the same CAGR. It can be argued that the k and ϕ parameters of the gravity model can be further optimized to mimic

Network	Gravity Model scaling parameter (k)	Total Peak Traffic (2021)[Tbps]	Assumed Market Penetration [%]	Peak Traffic per operator (2021) [Tbps]	CAGR [%]
Germany	100	127	25	31.75	26
Spain	10000	62	33	20.66	23
Sweden	100	22	100	22	24

Table 4: Traffic modelling parameters for the Gravity Model [43] and CISCO VNI forecast [38]

the VNI forecast. However, the proposed traffic model does not require any parameter optimization and is generic enough to be used for long-haul networks holding different graph properties. Finally, independent of this validation study, the results of the traffic model for the Spanish network show a similar trend to Fig.5 in Lopez *et. al.* [44], justifying the usage of this traffic model.

6.2. Planning Results

Now, we compare the results of the two deployment simulations in terms of aggregate network throughput, number of lightpaths deployed, underprovisioning, and lightpaths per band of operation.

Aggregate throughput is defined as the sum of the data rates of operational lightpaths in the network at a given planning period. As mentioned earlier, a lightpath is an end-to-end optical signal between a pair of transceivers (Flex-BVTs or CFP2-DCOs) at the source and destination, each having its own configuration. The aggregate throughput is compared with the requested aggregated traffic, which is defined as the sum of the demands between each source-destination pair in a given planning period.

The number of lightpaths is the cumulative count of in-operation lightpaths deployed in each planning period, and finally, the number of lightpaths per band shows how many lightpaths are added in the C, L, or S-band in each planning period. Using these four metrics, and the same RCSA algorithm, a multi-period planning study comparing the performance of Flex-BVT and CFP2-DCO on the three networks under study is carried out. The results for each of the networks are presented and discussed in detail.

From the throughput plots for the Germany network in Fig. 9, we observe

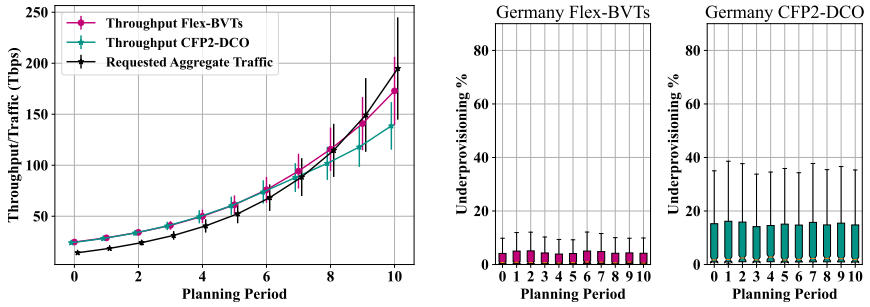

(a) Aggregate throughput (b) Underprovisioning

Figure 9: Throughput and Underprovisioning results for Germany network.

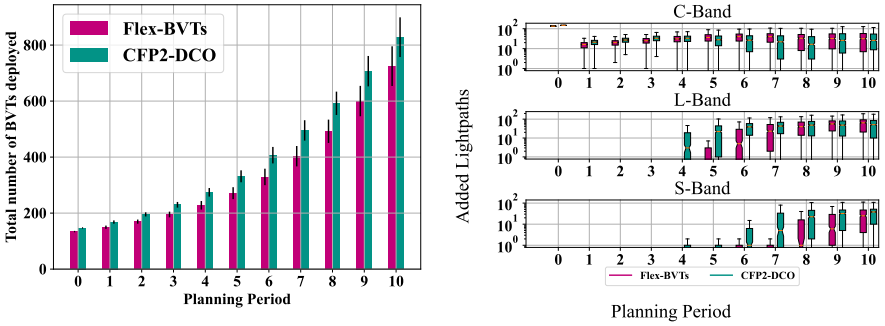

(a) Total deployed LPs (b) #LPs per band

Figure 10: Number of deployed LPs and the number of LPs in each of the bands for the Germany network.

that the Flex-BVT approach meets the requested aggregate traffic one year more as compared to the CFP2-DCO approach, with similar mean underprovisioning. However, CFP2-DCO deployment shows a higher third and fourth quartile in each planning year. This means that it is susceptible to having more lightpaths blocked due to high neighbouring channel interference, or due to band saturation. Compared to the CFP2-DCO approach, the Flex-BVT approach places at least 15% lesser lightpaths in the network, leading to a lesser number of devices.

As seen in Fig. 10b, S-Band is activated two years later in the Flex-BVT scenario, as compared to the CFP2-DCO scenario. The reason why the CFP2-DCO approach activates the L and S band in the fourth planning period is that the increase in traffic leads to high usage of spectral resources on a few links which carry many lightpaths (e.g. Frankfurt-Leipzig, Hannover-Frankfurt, and Hannover-Leipzig), leading to L-Band saturation in one planning period. This phenomenon is not observed for Flex-BVTs due to the usage of configurations with higher spectral efficiency.

From the results of the network study for Germany, it can be inferred that the Flex-BVT approach provides a similar or higher throughput than CFP2-DCO-based transparent IPoWDM deployment.

The Spanish network results, shown in Fig. 11 also highlight the advantages of the Flex-BVT approach with higher throughput and lower underprovisioning, as compared to the CFP2-DCO approach. Due to the star-like structure of the network, the links connecting the node Madrid get saturated earlier when using the CFP2-DCO approach. If the Flex-BVT approach is used instead of the CFP2-DCO approach, the L-Band and S-Band activation can be postponed by 1 and 2 years respectively.

Despite the change in topology, higher traffic, and longer average lightpath lengths (see Table 3), the Flex-BVT approach can provide 20% higher throughput, while placing approximately 10% lesser lightpaths on an average.

For the Swedish network, Fig. 12 shows a 15% higher underprovisioning on average for the CFP2-DCO approach, as compared to the Flex-BVT approach. In terms of throughput, both approaches can only meet the requested

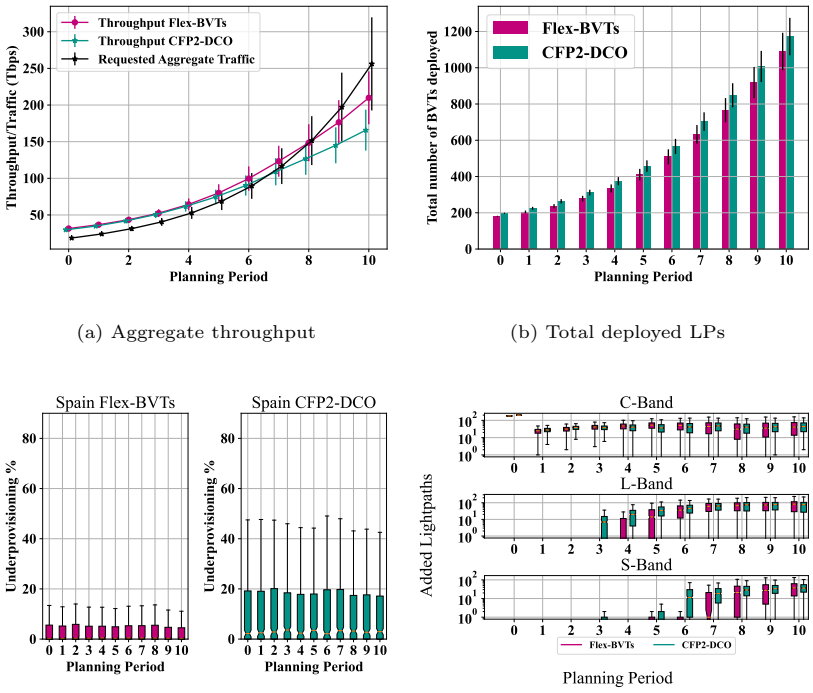

(a) Aggregate throughput

(b) Total deployed LPs

(c) Underprovisioning

(d) #LPs per band

Figure 11: Ten periods planning results for the Spanish network.

aggregate traffic up to the sixth planning period. Due to the longer average lightpath length in the networks and the point-to-point link structure of the network (Fig. 7), many demands cannot be satisfied and several links need to be upgraded to a multi-fiber setup, which is out of the scope of our network studies.

However, if the Flex-BVT approach is used, S-Band deployment in the Swedish network can be postponed by three planning periods, as compared to the CFP2-DCO approach.

As seen from the results, a Flex-BVT-based deployment outperforms the CFP2-DCO-based deployment for all the three core networks under study, highlighting its benefits of higher flexibility in configuration selection, higher spectral efficiency, and lower number of deployed devices in long-haul transparent optical networks.

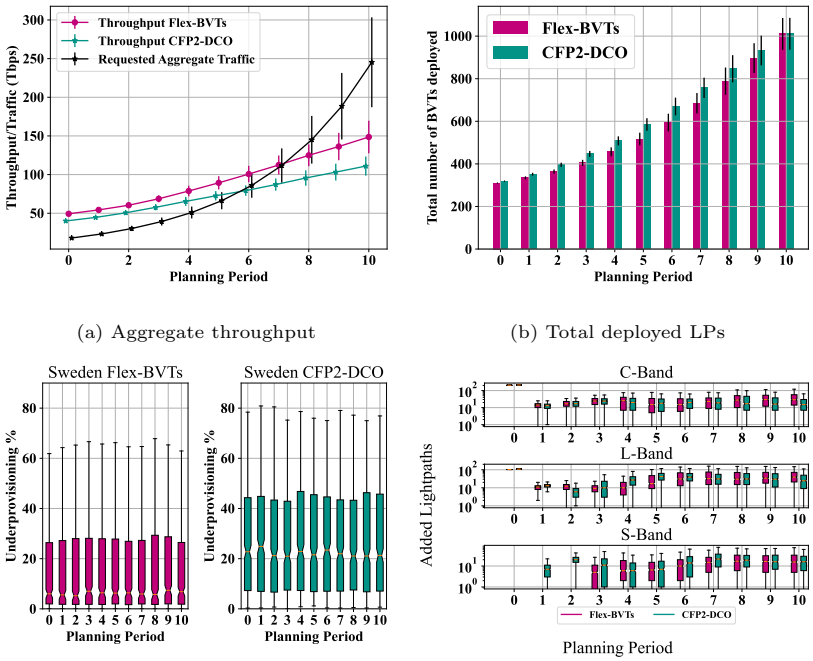

(a) Aggregate throughput

(b) Total deployed LPs

(c) Underprovisioning

(d) #LPs per band

Figure 12: Ten periods planning results for the Swedish network.

6.3. Cookie Cutter approach to Techno-economics

In business parlance, a 'cookie-cutter' approach is sometimes used to generalize steps, streamline processes and maintain uniformity. In a techno-economic analysis for networks, we employ a similar approach to arrive at estimates quickly and to give users an overview of the costs which need to be added to the network. Of course, this is not a substitute for careful and deliberate planning applied in the industry before creating commercial offerings. However, a quick estimate also helps in fastening the decision process by eliminating solutions with extremely high costs to benefits ratio. In our work, since we are comparing two different terminal deployments, and adding two additional bands, we compare the costs of adding extra equipment into the network. Using the component cost values provided in [45] and assuming that we have a deployed C-Band OLS, along with pre-existing core IP routers. It is important to note that the costs are normalized according to the cost of a 10G transceiver in the

Component	CAPEX (normalized C.U.)
Flex-BVT (100-600G)	17
CFP2-DCO Transceiver Card (100-400G)	12
Non-coherent IP Router	12 per 400G
Coherent optics IP Router (with CFP2-DCO cages)	20 per 400G
C, L-Band EDFA	2.8
Band splitter/combiner pair	0.2
S-Band TDFA	5.6

Table 5: Cookie-Cutter CAPEX values consolidated from [45, 46] for terminal and OLS equipment upgrade.

year 2020.

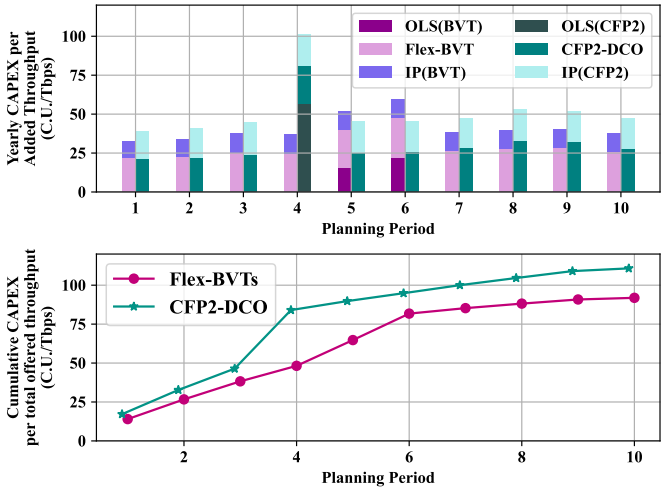

Figure 13: Per-period and cumulative CAPEX normalized to per-period and total offered throughput respectively, for German network.

The OLS upgrade can be planned in two steps. The first step is the replacement of pure C-Band EDFAs with ILA modules consisting of C-Band and L-Band EDFAs along with the placement of passive band splitters and combiners at each location. The second step is the installation of ILA modules consisting of S-Band TDFAs. This two-step approach enables operators to install and operate S-Band-based ILAs, only when a need for the same arises [47, 48]. Here, we do not undertake a cost sensitivity analysis in this approach, since this deviates from the cookie-cutter philosophy and requires taking into consideration

component customization. Therefore, for the CAPEX calculations, we take the mean values from the results generated in Sec. 6.2.

As seen in Table 5, CAPEX costs related to routers will increase, as the overall throughput in the network increases. It is clear from the throughput results of the three networks, that the Flex-BVT-based solution consistently places more throughput than the CFP2-DCO-based solution, thereby leading to a higher overall CAPEX. However, it must be noted that higher throughput would also lead to the ability of the network operator to offer services to more customers. Therefore, we normalized the yearly and cumulative CAPEX of each solution to the carried traffic. For this, we define two cost-per-bit metrics. The first metric, whose results are shown in the upper halves in Fig. 13 and Fig. 14 is the yearly CAPEX per yearly added traffic. This is simply the cost of new equipment in Cost Units (C.U.) normalized to the additional throughput added to the network in Tbps. The second metric, seen in the bottom halves of the same figures shows the cumulative CAPEX normalized to the total offered throughput of the network. The cumulative CAPEX in any given planning period is defined as the CAPEX costs accumulated from the first planning period to the current one. As the planning periods progress, it is possible that many transceivers can be upgraded to higher data rates to meet the requested traffic,

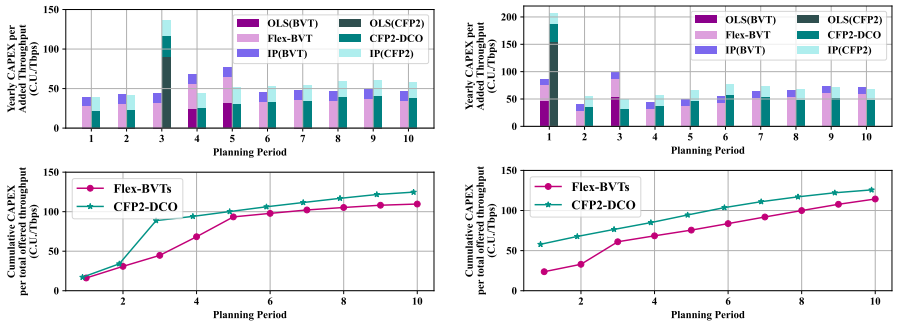

(a) Spain

(b) Sweden

Figure 14: Per-period and cumulative CAPEX normalized to per-period and total offered throughput respectively, for Spanish and Swedish networks.

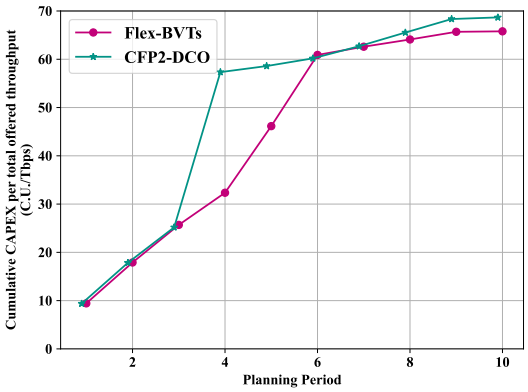

(a) Germany

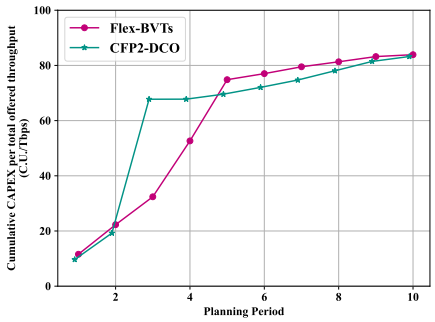

(b) Spain

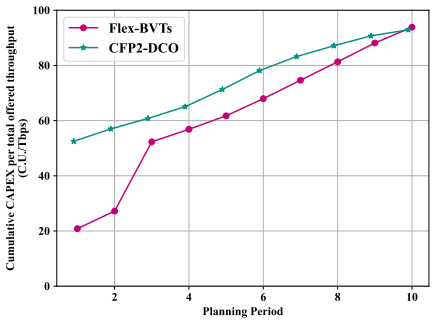

(c) Sweden

Figure 15: Cumulative CAPEX per offered throughput for the three networks under study, ignoring IP routing costs.

thereby avoiding the placement of new terminal equipment in the network.

This exercise helps not only to compare the differences in the cost per bit but also the benefits offered by the OLS and terminal upgrades. We assume higher IP routing costs due to the usage of coherent IP routers with CFP2-DCO cages as compared to grey-optics IP routers which can be either re-used or acquired at lesser costs as compared to their coherent counterparts [49]. As seen from Fig. 13, the per-component CAPEX normalized by the additional throughput added to the network shows that the Flex-BVT solution has a lower cost per bit as compared to the transparent IPoWDM-based solution. Although the costs of the terminal equipment are higher in the case of Flex-BVT, they are offset by

the usage of less expensive routers. Moreover, the absolute cost of OLS upgrade for both Flex-BVT and transparent IPoWDM scenarios is the same. However, since transparent IPoWDM carries lesser traffic, the cost per bit value turns out to be higher than the Flex-BVT case.

Specifically, at the end of the planning periods, the usage of the Flex-BVT solution provides an overall 12% reduction in the cost-per-bit, as compared to the transparent IPoWDM solution. More importantly, the cumulative CAPEX per bit is consistently lower in the case of the Flex-BVT solution, showing that if the offered traffic by the network operators is used to its maximum, Flex-BVTs indeed show promise in terms of higher flexibility, and lower cost-per-bit. As seen in Fig. 14, similar savings are seen in other networks, with the Spanish network showing an 11% reduction in the cost-per-bit and the Swedish network portraying a 6% reduction in the cost-per-bit.

For fairness in cost comparison, we also conduct a CAPEX study with only the OLS and Terminal costs. This is done to provide more insights into the cost components purely from a WDM perspective. For the three networks under study, we undertake a cost-per-bit analysis, using the costs provided in Table 5, but only considering the cost of OLS upgrades and additional terminals. The metric for comparison is Yearly CAPEX per total offered throughput in the network, which is measured in C.U. per Tbps.

From Fig. 15, we see that in most of the planning periods in all three networks, the Flex-BVT approach is either similar to or less expensive than the CFP2-DCO approach. The exceptions are planning periods 5-9 in the Spanish network and planning period 10 in the Swedish network. The reason for a lower CAPEX-per-bit for the CFP2-DCO approach is that from the fifth planning period, the L-Band starts saturating, leading to a lesser number of CFP2-DCO transceivers being added to the network, thereby also having an overall lower amount of throughput. However, towards the end of the planning periods, both the curves begin to converge, showing little to no economic advantage of investing in CFP2-DCO technologies for a long-haul transparent optical network deployment.

7. Conclusions

As research communities in Europe move towards standardization of 6G network services and deployment, an exponential increase in demands for high-bandwidth services to be carried over long distances is envisioned. Moreover, as 5G networks are already partially deployed in production environments, long-haul network operators must take timely decisions to upgrade core networks. These network upgrades can either be related to the choice of optical network terminal equipment or the choice of the type of OLS upgrades needed in the network.

To this end, we have proposed a novel traffic model, which simulates the expected traffic growth in core networks in a multi-period scenario. The model's stochastic nature allows it to provide inputs for different types of core networks, and to undertake a network planning and techno-economic study. We also propose a multi-period Routing, Configuration, and Spectrum Assignment (RCSA) algorithm which takes as input demands modelled by the novel traffic model, and provides results in terms of network throughput, number of lightpaths (total and per-band), and the per-period underprovisioning.

Using the traffic model and the RCSA algorithm, we conduct a multi-period planning study on the German, Spanish, and Swedish networks. This study compares differences between multi-band deployments based on highly flexible bandwidth variable (Flex-BVT) transceivers, versus transparent IP over WDM transceivers (IPoWDM) deployments that use CFP2-DCOs. Results show that the Flex-BVT approach places up to 15% lower lightpaths into the network while carrying up to 20% higher traffic. Using a 'cookie-cutter' CAPEX calculation approach, we also show that the cost-per-bit of deploying bandwidth variable transceivers is up to 12% lower, as compared to the CFP2-DCO approach under study.

Additionally, a cost-per-bit study comparing the two approaches only from the OLS and terminal costs perspective shows that the Flex-BVT approach has either similar or lower cost per bit in 80% of the planning periods for the three

networks in the study. Future work will include extending the techno-economic study to include operating expenditures and extending the network planning study to include multi-fiber as well as regenerator-based approaches.

8. Acknowledgments

This work has been partially funded in the framework of the CELTIC-NEXT project AI-NET-PROTECT (Project ID C2019/3-4) by the German Federal Ministry of Education and Research (**#16KIS1279K**). Carmen Mas-Machuca acknowledges the support of the Federal Ministry of Education and Research of Germany (BMBF) in the programme "Souverän. Digital. Vernetzt." joint project 6G-life (**#16KISK002**).

References

[1] European-Commission, *Upcoming report on the rollout of 5G in the EU*, https://www.eca.europa.eu/en/Pages/NewsItem.aspx?nid=16334, Accessed: 2022-04-24.

[2] D. Goovaerts, *Altice USA loses 13K broadband subs as it waits for fiber growth*, https://www.fiercetelecom.com/broadband/altice-usa-loses-13k-broadband-subs-it-waits-fiber-growth, Accessed: 2022-04-24.

[3] K. Hill, *Network costs are going up, says Nokia CEO*, https://www.rcrwireless.com/20220429/network-infrastructure/network-costs-are-going-up-says-nokia-ceo, Accessed: 2022-04-24.

[4] telecompaper, *DB Broadband to lease out fibre*, https://www.telecompaper.com/share/news/--1405680, Accessed: 2022-04-24.

[5] ADVA, *TeraFlex™*, https://www.adva.com/en/products/open-optical-transport/fsp-3000-open-terminals/teraflex, Accessed: 2022-04-24.

[6] Acacia, *CFP2-DCO Product Family*, https://acacia-inc.com/product/cfp2/, Accessed: 2022-04-24.

[7] A. Ferrari, E. Virgillito, V. Curri, Band-division vs. space-division multiplexing: A network performance statistical assessment, Journal of Lightwave Technology 38 (5) (2020) 1041–1049. doi:10.1109/JLT.2020.2970484.

[8] B. Shariati, J. M. Rivas-Moscoso, D. Klonidis, I. Tomkos, S. Ben-Ezra, F. Jiménez, D. M. Marom, P. S. Khodashenas, J. Comellas, L. Velasco, Options for Cost-effective Capacity Upgrades in Backbone Optical Networks, in: 2016 21st European Conference on Networks and Optical Communications (NOC), 2016, pp. 35–40. doi:10.1109/NOC.2016.7506982.

[9] R. Freund, L. Molle, F. Raub, C. Caspar, M. Karkri, C. Weber, Triple-(S/C/L)-band WDM transmission using erbium-doped fibre amplifiers, in: 2005 31st European Conference on Optical Communication, ECOC 2005, Vol. 1, 2005, pp. 69–70 vol.1. doi:10.1049/cp:20050382.

[10] A. H. Gnauck, G. Charlet, P. Tran, P. J. Winzer, C. R. Doerr, J. C. Centanni, E. C. Burrows, T. Kawanishi, T. Sakamoto, K. Higuma, 25.6-Tb/s C+L-Band Transmission of Polarization-Multiplexed RZ-DQPSK Signals, in: Optical Fiber Communication Conference and Exposition and The National Fiber Optic Engineers Conference, Optica Publishing Group, 2007, p. PDP19.

[11] A. Sano, H. Masuda, T. Kobayashi, M. Fujiwara, K. Horikoshi, E. Yoshida, Y. Miyamoto, M. Matsui, M. Mizoguchi, H. Yamazaki, Y. Sakamaki, H. Ishii, Ultra-High Capacity WDM Transmission Using Spectrally-Efficient PDM 16-QAM Modulation and C- and Extended L-Band Wideband Optical Amplification, Journal of Lightwave Technology 29 (4) (2011) 578–586. doi:10.1109/JLT.2011.2107030.

[12] N. Sambo, P. Castoldi, A. D'Errico, E. Riccardi, A. Pagano, M. S. Moreolo, J. M. Fàbrega, D. Rafique, A. Napoli, S. Frigerio, E. H. Salas, G. Zervas,

M. Nolle, J. K. Fischer, A. Lord, J. P. F.-P. Giménez, Next generation sliceable bandwidth variable transponders, IEEE Communications Magazine 53 (2) (2015) 163–171. doi:10.1109/MCOM.2015.7045405.

[13] M. Jinno, H. Takara, Y. Sone, K. Yonenaga, A. Hirano, Multiflow optical transponder for efficient multilayer optical networking, IEEE Communications Magazine 50 (5) (2012) 56–65. doi:10.1109/MCOM.2012.6194383.

[14] J. Zhang, Y. Ji, M. Song, Y. Zhao, X. Yu, J. Zhang, B. Mukherjee, Dynamic traffic grooming in sliceable bandwidth-variable transponder-enabled elastic optical networks, Journal of Lightwave Technology 33 (1) (2015) 183–191.

[15] P. Soumplis, K. Christodoulopoulos, M. Quagliotti, A. Pagano, E. Varvarigos, Network planning with actual margins, Journal of Lightwave Technology 35 (23) (2017) 5105–5120.

[16] R. Eisenach, Understanding 400zr/openzr+/400zr+ Optics, https://www.lightwaveonline.com/optical-tech/transmission/article/14188934/understanding-400zropenzr400zr-optics Accessed: 2022-04-20.

[17] T. Zami, B. Lavigne, O. B. Pardo, Benchmarking of Opaque Versus Transparent Core WDM Networks Featuring 400ZR+ QSFP-DD or CFP2 Interfaces, in: 2020 European Conference on Optical Communications (ECOC), 2020, pp. 1–4. doi:10.1109/ECOC48923.2020.9333414.

[18] T. Zami, B. Lavigne, Optimal deployments of 400 Gb/s multihaul CFP2-DCO transponders in transparent IPoWDM core networks, in: Optical Fiber Communication Conference (OFC) 2022, Optica Publishing Group, 2022, p. Th1F.1. doi:10.1364/OFC.2022.Th1F.1.

[19] S. Melle, *Building IP-optical solutions that are more than the sum of their parts*, https://nokia.ly/3dR3d4D, Accessed: 2022-04-24.

[20] B. Correia, R. Sadeghi, E. Virgillito, A. Napoli, N. Costa, J. Pedro, V. Curri, Networking performance of power optimized c+l+s multiband transmission, in: GLOBECOM 2020 - 2020 IEEE Global Communications Conference, 2020, pp. 1–6. doi:10.1109/GLOBECOM42002.2020.9322068.

[21] R. Sadeghi, B. Correia, E. Virgillito, A. Napoli, N. Costa, J. Pedro, V. Curri, Cost-effective capacity increase of deployed optical networks to support the future internet: the multi-band approach, in: 2021 12th International Conference on Network of the Future (NoF), 2021, pp. 1–7. doi:10.1109/NoF52522.2021.9609888.

[22] T. Ahmed, S. Rahman, M. Tornatore, X. Yu, K. Kim, B. Mukherjee, Dynamic Routing and Spectrum Assignment in Co-Existing Fixed/Flex-Grid Optical Networks, in: 2018 IEEE International Conference on Advanced Networks and Telecommunications Systems (ANTS), 2018, pp. 1–3. doi:10.1109/ANTS.2018.8710140.

[23] E. E. Moghaddam, H. Beyranvand, J. A. Salehi, Routing, spectrum and modulation level assignment, and scheduling in survivable elastic optical networks supporting multi-class traffic, Journal of Lightwave Technology 36 (23) (2018) 5451–5461. doi:10.1109/JLT.2018.2874820.

[24] G. Choudhury, D. Lynch, G. Thakur, S. Tse, Two use cases of machine learning for SDN-enabled IP/optical networks: traffic matrix prediction and optical path performance prediction [invited], Journal of Optical Communications and Networking 10 (10) (2018) D52–D62. doi:10.1364/JOCN.10.000D52.

[25] L. Velasco, A. Castro, M. Ruiz, G. Junyent, Solving routing and spectrum allocation related optimization problems: From off-line to in-operation flex-grid network planning, Journal of Lightwave Technology 32 (16) (2014) 2780–2795. doi:10.1109/JLT.2014.2315041.

[26] X. Chen, J. Guo, Z. Zhu, R. Proietti, A. Castro, S. J. B. Yoo, Deep-RMSA: A Deep-Reinforcement-Learning Routing, Modulation and Spec-

trum Assignment Agent for Elastic Optical Networks, in: 2018 Optical Fiber Communications Conference and Exposition (OFC), 2018, pp. 1–3.

[27] C. Natalino, P. Monti, The optical RL-Gym: An open-source toolkit for applying reinforcement learning in optical networks, in: 2020 22nd International Conference on Transparent Optical Networks (ICTON), 2020, pp. 1–5. doi:10.1109/ICTON51198.2020.9203239.

[28] X. Zhou, W. Lu, L. Gong, Z. Zhu, Dynamic RMSA in elastic optical networks with an adaptive genetic algorithm, in: 2012 IEEE Global Communications Conference (GLOBECOM), 2012, pp. 2912–2917. doi:10.1109/GLOCOM.2012.6503559.

[29] J. Pedro, N. Costa, S. Pato, Optical transport network design beyond 100 Gbaud [Invited], J. Opt. Commun. Netw. 12 (2) (2020) A123–A134. doi:10.1364/JOCN.12.00A123.

[30] S. K. Patri, A. Autenrieth, J.-P. Elbers, C. Mas-Machuca, Planning optical networks for unexpected traffic growth, in: 2020 European Conference on Optical Communications (ECOC), 2020, pp. 1–4. doi:10.1109/ECOC48923.2020.9333215.

[31] A. Varasteh, S. K. Patri, A. Autenrieth, C. Mas-Machuca, Evaluation of Lightpath Deployment Strategies in Flexible-Grid Optical Networks, in: 2021 International Conference on Optical Network Design and Modeling (ONDM), 2021, pp. 1–6. doi:10.23919/ONDM51796.2021.9492493.

[32] D. Uzunidis, E. Kosmatos, C. Matrakidis, A. Stavdas, A. Lord, Strategies for upgrading an operator's backbone network beyond the c-band: Towards multi-band optical networks, IEEE Photonics Journal 13 (2) (2021) 1–18. doi:10.1109/JPHOT.2021.3054849.

[33] C. Mas-Machuca, S. K. Patri, S. Amjad, Long-term capacity planning in flexible optical transport networks, in: 2022 Optical Fiber Communications Conference and Exhibition (OFC), 2022, pp. 1–3.

[34] B. Correia, R. Sadeghi, E. Virgillito, A. Napoli, N. Costa, J. ao Pedro, V. Curri, Power control strategies and network performance assessment for C+L+S multiband optical transport, J. Opt. Commun. Netw. 13 (7) (2021) 147–157. doi:10.1364/JOCN.419293.

[35] A. R. Chraplyvy, Limitations on lightwave communications imposed by optical-fiber nonlinearities, Journal of Lightwave Technology 8 (10) (1990) 1548–1557.

[36] D. Semrau, L. Galdino, E. Sillekens, D. Lavery, R. I. Killey, P. Bayvel, *Modulation format dependent, closed-form formula for estimating nonlinear interference in S+C+L band systems*, in: 45th European Conference on Optical Communication (ECOC 2019), 2019, pp. 1–4. doi:10.1049/cp.2019.0892.

[37] A. Janota, T. Gould, M. Gully, *Equinix Internet Exchange® Traffic Sustains Growth Across Regions*, https://bit.ly/3Tl1hSi, Accessed: 2022-04-24.

[38] CISCO, *CISCO Global VNI Forecast Highlights*, https://www.cisco.com/c/dam/m/en_us/solutions/service-provider/vni-forecast-highlights/pdf/Global_2021_Forecast_Highlights.pdf, Accessed: 2022-08-12.

[39] A. Soule, A. Nucci, R. Cruz, E. Leonardi, N. Taft, How to identify and estimate the largest traffic matrix elements in a dynamic environment, in: Proceedings of the joint international conference on Measurement and modeling of computer systems, 2004, pp. 73–84.

[40] A. Souza, R. Sadeghi, B. Correia, N. Costa, A. Napoli, V. Curri, J. Pedro, J. Pires, Optimal Pay-As-You-Grow Deployment on S+C+L Multi-band Systems, in: 2022 Optical Fiber Communications Conference and Exhibition (OFC), 2022, pp. 1–3.

[41] Github, *Physical Network Information*, www.github.com/SaiPatri/PhyNWInfo, Accessed: 2022-04-24.

[42] *Internet Topology Zoo*, http://www.topology-zoo.org/dataset.html, Accessed: 2022-04-24.

[43] A. Dwivedi, R. Wagner, Traffic model for usa long-distance optical network, in: Optical Fiber Communication Conference. Technical Digest Postconference Edition. Trends in Optics and Photonics Vol.37 (IEEE Cat. No. 00CH37079), Vol. 1, 2000, pp. 156–158 vol.1. doi:10.1109/OFC.2000.868400.

[44] V. Lopez, B. Zhu, D. Moniz, N. Costa, J. Pedro, X. Xu, A. Kumpera, L. Dardis, J. Rahn, S. Sanders, Optimized Design and Challenges for C&L Band Optical Line Systems, Journal of Lightwave Technology 38 (5) (2020) 1080–1091. doi:10.1109/JLT.2020.2968225.

[45] J. Alberto Hernandez, M. Quagliotti, L. Serra, L. Luque, R. Lopez da Silva, A. Rafel, O. Gonzalez de Dios, V. Lopez, A. Eira, R. Casellas, A. Lord, J. Pedro, D. Larrabeiti, Comprehensive model for technoeconomic studies of next-generation central offices for metro networks, Journal of Optical Communications and Networking 12 (12) (2020) 414–427. doi:10.1364/JOCN.402167.

[46] R. K. Jana, A. Mitra, A. Pradhan, K. Grattan, A. Srivastava, B. Mukherjee, A. Lord, When is operation over C + L bands more economical than multifiber for capacity upgrade of an optical backbone network?, in: 2020 European Conference on Optical Communications (ECOC), 2020, pp. 1–4. doi:10.1109/ECOC48923.2020.9333276.

[47] M. Cantono, R. Schmogrow, M. Newland, V. Vusirikala, T. Hofmeister, Opportunities and challenges of c+ l transmission systems, Journal of Lightwave Technology 38 (5) (2020) 1050–1060.

[48] K. Jordan, *The benefits of an integrated C&L-band photonic line system*, https://www.ciena.com/insights/articles/The-benefits-of-an-integrated-CL-band-photonic-line-system.html Accessed: 2022-08-02.

[49] I. Busi, *IP + Optical: The Mainstream Solution for the 400G Era*, https://blog.huawei.com/2022/07/04/ip-optical-mainstream-solution-400g/, Accessed: 2022-08-17.